



Published in final edited form as:

*Nat Med.* 2011 April ; 17(4): 454–460. doi:10.1038/nm.2334.

## Potent Inhibition of Heterotopic Ossification by Nuclear Retinoic Acid Receptor $\gamma$ Agonists

Kengo Shimono<sup>1</sup>, Wei-en Tung<sup>1</sup>, Christine Macolino<sup>1</sup>, Amber Hsu-Tsai Chi<sup>1</sup>, Johanna J. Didizian<sup>1</sup>, Christina Mundy<sup>1</sup>, Roshantha A. Chandraratna<sup>2</sup>, Yuji Mishina<sup>3</sup>, Motomi Enomoto Iwamoto<sup>1</sup>, Maurizio Pacifici<sup>1</sup>, and Masahiro Iwamoto<sup>1</sup>

<sup>1</sup> Department of Orthopaedic Surgery, Thomas Jefferson University College of Medicine, Philadelphia, Pennsylvania 19107, USA

<sup>2</sup> NuRx Pharmaceuticals Inc., Irvine, California 92618, USA

<sup>3</sup> School of Dentistry, University of Michigan, Ann Arbor, Michigan 48109, USA

### Abstract

Heterotopic ossification (HO) consists of ectopic bone formation within soft tissues following surgery or trauma and can have debilitating consequences, but no definitive cure is available. Here we show that HO was essentially prevented in mice receiving nuclear retinoic acid receptor  $\gamma$  (RAR $\gamma$ ) agonists. Side effects were minimal, and there was no significant rebound effect. To uncover mechanisms, mesenchymal stem cells were treated with RAR $\gamma$  agonist and transplanted into nude mice. Whereas control cells formed ectopic bone masses, the RAR $\gamma$  agonist-pretreated cells did not, suggesting that they had lost their skeletogenic potentials. Indeed, the cells became unresponsive to rBMP-2 and exhibited reduction of Smad1/5/8 phosphorylation and overall Smad levels. As importantly, the RAR $\gamma$  agonists blocked HO in transgenic mice expressing constitutive-active ALK2<sup>Q207D</sup> mutant that is related to ALK2<sup>R206H</sup> found in Fibrodysplasia Ossificans Progressiva patients. The data indicate that the RAR $\gamma$  agonists are potent inhibitors of HO and could also be as effective against congenital HO.

Heterotopic ossification (HO) is a potentially severe pathology in which ectopic bone forms within muscles and connective tissues and near blood vessels or nerves. Over 10% of patients undergoing invasive surgeries can develop HO<sup>1–3</sup>, and a staggering 65% of seriously wounded soldiers develop the disease as well<sup>4</sup>, causing chronic pain, prosthesis fitting problems, deep venous thrombosis, limited motion or other complications. Though HO pathogenesis remains unclear, it is generally agreed that the inciting events—be it trauma, surgery, deep burns or protracted immobilization—induce local inflammation<sup>5,6</sup>. This is followed by recruitment of skeletal progenitor cells that differentiate into chondrocytes,

Users may view, print, copy, download and text and data-mine the content in such documents, for the purposes of academic research, subject always to the full Conditions of use: [http://www.nature.com/authors/editorial\\_policies/license.html#terms](http://www.nature.com/authors/editorial_policies/license.html#terms)

Correspondence should be addressed to M.I. (IwamotoM@email.chop.edu) or M.P. (PacificiM@email.chop.edu). Current address for K.S., W.T., J.J.D., M.E.I., M.P. and M.I. is The Children's Hospital of Philadelphia, Division of Orthopaedic Surgery, Philadelphia, Pennsylvania 19104, USA.

### AUTHOR CONTRIBUTIONS

M.I. and M.P. directed the project. K.S., W.T., C.M., A. H-S. C., J.J., C.M., and M. E.-I. performed experiments and analyzed data and participated in experimental design. R.A.C. provided expertise on retinoid biology. M.P., K.S. and M.I. wrote the manuscript.

undergo hypertrophy and are replaced by endochondral bone. Patients with the rare congenital condition Fibrodysplasia Ossificans Progressiva (FOP) develop extensive HO that is also incited by trauma and inflammation<sup>7</sup>, is aggressive and often fatal and is propelled by an activating mutation in the BMP type I receptor, activin receptor-like kinase-2 (ALK2<sup>R206H</sup>)<sup>8</sup>. Given HO etiology, current therapeutic treatments aim to target different pathogenic steps, but success has varied and is far from ideal<sup>9,10</sup>. A recent study tested a selective inhibitor of BMP type I receptor kinases in transgenic mice<sup>11</sup> that express a strong constitutive-active ALK2<sup>Q207D</sup> mutant originally characterized by Zhang et al.<sup>12</sup>, and found some inhibition of muscle-associated HO<sup>13</sup>. Using a standard subcutaneous HO mouse model, we tested a selective agonist for the nuclear retinoic acid receptor  $\alpha$  (RAR $\alpha$ )<sup>14</sup>. The rationale was based on the fact that retinoid signaling is a strong inhibitor of chondrogenesis<sup>15</sup> and that unliganded RAR transcriptional repressor activity—possibly involving RAR $\alpha$ - is needed for chondrogenic differentiation<sup>16,17</sup>. The RAR $\alpha$  agonist did inhibit HO, but not completely. To further explore a retinoid agonist-based therapy for HO, we considered the fact that another RAR family member with distinct characteristics<sup>18</sup> - RAR $\gamma$ - is expressed in chondrogenic cells<sup>17</sup> and chondrocytes<sup>19</sup> where it also operates as an unliganded transcriptional repressor<sup>20</sup>. Hence, a RAR $\gamma$  agonist-based anti-HO therapy could actually be more effective because it would target both chondrogenic cells and chondrocytes. The data presented here support this enticing possibility.

## RESULTS

### RAR $\gamma$ agonists block chondrogenesis

To test whether RAR $\gamma$  agonists inhibit chondrogenesis, micromass cultures of E11.5 mouse embryo limb mesenchymal cells were treated with the synthetic selective RAR $\gamma$  agonist NRX204647<sup>20,21</sup>. For comparison, companion cultures were treated with all-*trans*-retinoic acid (RA), the active natural vitamin A derivative that is a pan-agonist, activates every RAR (RAR $\alpha$ , RAR $\beta$  and RAR $\gamma$ ) and is well known for its anti-chondrogenic action<sup>15</sup>. Whereas numerous Alcian blue-positive cartilaginous nodules formed in control cultures (Fig. 1a), few if any formed in NRX204647-treated cultures; inhibition was actually greater than that elicited by comparable RA doses (Fig. 1a). To test RAR $\gamma$  relevance in regulation of chondrogenesis, we prepared micromass cultures with limb mesenchymal cells from E11.5 RAR $\gamma$ -null embryos that still express RAR $\alpha$  and RAR $\beta$ <sup>20</sup>. Interestingly, treatment with RA failed to inhibit chondrogenesis in these RAR $\gamma$ -null cultures (Fig. 1b). To verify the apparent centrality of RAR $\gamma$ , we prepared micromass cultures with limb mesenchymal cells isolated from double RAR $\alpha$ /RAR $\beta$ -null embryos (that still express RAR $\gamma$ ) and treated them with RA; analysis of conditional gene deletion and genotyping is described in Supplementary Fig. 1. Indeed, chondrogenesis was fully suppressed by RA in these double mutant cultures as was in companion WT cultures (Fig. 1c). Thus, RAR $\gamma$  agonists can block chondrogenic differentiation, and RAR $\gamma$  appears to exert a preponderant role in the control of chondrogenesis.

### RAR $\gamma$ agonists inhibit trauma-induced HO

To determine whether RAR $\gamma$  agonists inhibit HO, we used a standard mouse model that combines local trauma and implantation of a skeletogenic factor<sup>22</sup>. In such models<sup>14</sup>,

progenitor cells are recruited to the injured site and form cartilage by day 5 or 6; cartilage undergoes hypertrophy and is replaced by endochondral bone by day 10–14. Thus, we created a small microsurgical pouch in 2 month-old female mouse calf muscles and inserted a collagen sponge containing 1  $\mu$ g of recombinant BMP-2 serving as a skeletogenic factor. Starting on day 1, mice received daily doses of NRX204647 (1.2 mg per kg body weight per day), RA (12 mg per kg body weight per day) or corn oil (vehicle control) by gavage for 12 to 14 days. Large ectopic mineralized tissue masses formed in vehicle-treated mice at the operated site near tibia and fibula by day 14 (Fig. 1d, arrow in top row left panel), but formation of such tissues was significantly reduced in RA-treated mice and essentially prevented in RAR $\gamma$  agonist-treated mice (Fig. 1d). Masson's trichrome (MT) and Alcian blue (AB) staining showed that ectopic masses in control mice contained abundant cartilage, endochondral bone and marrow (Fig. 1d) and proliferative cells (Supplementary Fig. 2), but all these tissues were diminished in RA-treated mice and were essentially absent in RAR $\gamma$  agonist-treated mice (Fig. 1d) and the number of proliferative cells was lower as well (Supplementary Fig. 2). In good agreement, the bone markers osteocalcin (OC) and tartrate-resistant alkaline phosphatase (TRAP) were prominent in control ectopic tissues, were clearly reduced in RA-treated mice and were undetectable in RAR $\gamma$  agonist-treated mice (Fig. 1d). Identical results were obtained with subcutaneous HO model (Fig. 1e) we used previously<sup>14</sup>. Because the drugs are given systemically, they could have unwanted side effects. However, no obvious changes were seen in food intake and blood chemistry (Supplementary Fig. 3) and trabecular bone density (Supplementary Fig. 4). Exceptions were skin redness and loss of some whiskers in mice receiving the highest RA doses (12 mg per kg body weight per day) and a transient delay in long bone fracture repair in mice receiving the highest NRX204647 dose (1.2 mg per kg body weight per day) (Supplementary Fig. 3).

### Drug class effect by RAR $\gamma$ agonists

Synthetic RAR $\gamma$  agonists differ in chemical and physical characteristics, backbone structure and effectiveness<sup>21, 23–25</sup>. Thus, we compared the anti-HO activity of NRX204647 with that of CD1530 and R667 (Fig. 2a) to determine whether HO inhibition is a drug class effect. Two month-old mice were implanted with 1  $\mu$ g rBMP-2 in 250  $\mu$ l Matrigel subcutaneously to induce HO<sup>14</sup>, and mice received the indicated daily doses of NRX204647, CD1530<sup>26</sup> or R667<sup>27</sup> by gavage. For comparison, companion groups of mice received daily doses of: (i) corn oil (vehicle control); (ii) retinol that is the largely inert precursor of natural active retinoids<sup>28</sup>; (iii) RA; (iv) 13-*cis*-retinoic acid (13-*cis*-RA) that was tested for HO prevention in FOP patients<sup>29</sup>; or (v) the RAR $\alpha$  agonist NRX195183 that we tested in HO mouse model previously<sup>14</sup>. Large subcutaneous ectopic masses of vascularized and mineralized tissues formed in controls, but their formation was dose-dependently inhibited by each RAR $\gamma$  agonist tested as indicated by soft X-ray, histology and  $\mu$ CT-based quantification of bone volume/total volume (BV/TV) ratios (Fig. 2b,c). Because all the RAR $\gamma$  agonists were effective, they were used interchangeably in subsequent experiments. In line with above data and our previous work, the pan-agonist RA and the RAR $\alpha$  agonist NRX185183 inhibited HO as well, but their effectiveness was partial and required high doses<sup>30</sup> (Fig. 2b). Not surprisingly, retinol had no effect, but unexpectedly, 13-*cis*-RA had a slight and consistent

stimulatory effect (Fig. 2b), possibly accounting for flares up seen in certain FOP patients treated with it<sup>29</sup>.

To verify specificity of RAR $\gamma$  agonist action, we induced subcutaneous HO in RAR $\gamma$ -null mice and companion heterozygous RAR $\gamma^{+/-}$  and wild type mice, and treated them with CD1530 or NRX204647 for 12 to 14 days. The agonists did block HO in wild type and heterozygous mice as expected, but not in RAR $\gamma$ -null mice (Fig. 2d). To determine whether HO would re-start following stoppage of drug treatment (a phenomenon usually referred to as “rebound effect”), we induced subcutaneous HO and treated the mice with CD1530 or corn oil (control) for 10 days. A few control and treated mice were sacrificed at that point, and the remaining mice were withdrawn from drug treatment and examined over time. The ectopic tissues grew in control mice, but minimally in CD1530-treated mice indicative of no rebound effect (Fig. 2e). Thus, we tested the RAR $\alpha$  agonist NRX195183 and observed a rebound effect in this case (Fig. 2e). Lastly, we asked whether the RAR $\gamma$  agonists would be effective against HO even if treatment were not to start immediately, providing insights into the “window of opportunity”. Thus, treatment with CD1530 or corn oil was started on day 6 (corresponding to the chondrogenic phase of HO) and continued for 6 to 8 days. The RAR $\gamma$  agonist was still able to block HO (Fig. 2f). However, when treatment was delayed until day 12 (corresponding to the osteogenic phase), the RAR $\gamma$  agonist had minimal to no effects (Supplementary Fig. 5). Together, the data indicate that the agonists block HO by preventing chondrogenic cell differentiation and cartilage formation, but have minimal effects once bone has formed.

### RAR $\gamma$ agonists prevent HO in ALK2<sup>Q207D</sup> mice

Congenital HO in FOP patients is driven by the ALK2<sup>R206H</sup> mutant<sup>8</sup> that has mild basal constitutive activity but becomes hyper-active upon ligand binding<sup>31</sup>. To determine whether RAR $\gamma$  agonists could be effective against congenital HO, we prepared an expression vector encoding the strongly constitutive-active ALK2<sup>Q207D</sup> mutant originally shown to induce chondrogenesis and endochondral ossification in chick<sup>12</sup>, and expressed it in ATDC5 mesenchymal cells along with BMP signaling reporter plasmid Id1-luc<sup>32</sup>. Cells were then treated with different CD1530 doses and luciferase activity was measured after 24 hrs. Reporter activity markedly increased in ALK2<sup>Q207D</sup>-expressing cells compared to empty vector control cells (Fig. 3a), but such increase was significantly inhibited by CD1530 treatment (Fig. 3a). To test effectiveness *in vivo*, we used the conditional ALK2<sup>Q207D</sup> transgenic mice in which effectiveness of a BMP type I receptor kinase inhibitor against FOP-like HO was tested recently<sup>13</sup>. Mice received a local intramuscular injection of adeno-Cre in a hind limb and were then treated with CD1530 or vehicle. Whereas massive HO developed in vehicle-treated mice, HO was essentially absent in CD1530-treated mice (Fig. 3b,c). To verify data, mice were injected with Alizarin complexon prior to sacrifice. Whereas abundant AR-staining tissue was appreciable in vehicle-treated animals (Fig. 3d, middle bottom panel), there was no obvious AR-positive tissue in CD1530-treated mice (Fig. 3d, right bottom panel).

### RAR $\gamma$ agonists reduce BMP signaling

To clarify the mechanisms by which the RAR $\gamma$  agonists inhibit HO, ADTC5 cell cultures were co-transfected with the Id1-luc reporter plasmid and treated with different CD1530 concentrations (0 to 100 nM) in absence or presence of exogenous rBMP-2 (100 ng ml<sup>-1</sup>) for 24 hrs. Luciferase activity was stimulated over 10-fold by rBMP-2 treatment, but such increase was counteracted by CD1530 co-treatment (Fig. 4a) or NRX204647 (not shown). BMPs transmit signals via transient phosphorylation of Smad1, Smad5 and Smad8<sup>33</sup>. Immunoblot analysis using p-Smad1/5/8 antibodies showed that in control cells Smad phosphorylation was in fact already strong by 30 min of BMP-2 treatment (100 ng ml<sup>-1</sup>), peaked at 1 hr and returned to basal levels by 3 hrs (Fig. 4b, top panel). Co-treatment with CD1530 reduced the levels of p-Smad proteins by over 80% as estimated by imaging quantification and normalization to  $\alpha$ -tubulin levels (Fig. 4b, top panel). CD1530 treatment could have provoked such drop in p-Smad levels by affecting mechanisms involved in signal transduction and Smad phosphorylation and/or reducing the overall steady-state levels of (unphosphorylated) Smad proteins. To test the latter possibility, we processed identical immunoblots with antibodies to Smad1. Indeed, there was a drastic reduction in overall Smad1 amounts in CD1530-treated cells, while these levels remained essentially unchanged in companion control cells (Fig. 4b, lower panel). The decreases in Smad1 levels were even appreciable by immunofluorescence staining (Fig. 4c). In control cells, Smad1 was largely if not exclusively confined to the cytoplasm, but relocated to the nucleus upon rBMP-2 treatment as expected (Fig. 4c, left and middle panels). In cells treated with CD1530 for 24 hrs (in absence or presence of rBMP-2), there was little if any appreciable Smad1 in cytoplasm or nucleus (Fig. 4c, right panels). In addition, similar decreases were seen in overall levels of Smad5 and regulatory Smad4 in CD1530-treated cells (Fig. 4d). What could have led to such significant reductions in Smad protein levels? A likely possibility is that the proteins were shunted toward degradation<sup>34</sup>. To test it, cells were treated with 1  $\mu$ M CD1530 in absence or presence of proteasome inhibitors AW9155 or PI-108 for 6 hrs and the resulting cell lysates were probed by immunoblot. Clearly, whereas treatment with CD1530 led to the expected Smad1 level drop, this response was mitigated by co-treatment with either proteasome inhibitor (Fig. 4e).

### RAR $\gamma$ agonists alter cell differentiation potentials

The marked reduction in steady-state levels of Smad1, Smad4 and Smad5 caused by RAR $\gamma$  agonist treatment suggested that the progenitor cells could have lost their lineage assignment and skeletogenic potentials. To test this interesting possibility, we treated ADTC5 cells in monolayer with 1  $\mu$ M CD1530 or vehicle for 2 days. Control and CD1530-treated cells were then detached, rinsed, reseeded in multiwell cultures, grown in absence or presence of 100 ng ml<sup>-1</sup> rBMP-2 for an additional 7 days (without further CD1530 treatment) and finally assessed for chondrogenic differentiation. As expected, control cells underwent differentiation upon rBMP-2 treatment and stained strongly with Alcian blue (a measure of chondrocyte differentiation and cartilage matrix accumulation) and alkaline phosphatase activity (a measure of chondrocyte maturation) (Figs. 5a-5b). However, CD1530-pretreated cells did not (Figs. 5a-5b). To verify data, we repeated the experiments with bone marrow-derived mesenchymal stem cells (MSCs) isolated from a reporter mouse line<sup>35</sup>. Whereas control cells treated with rBMP-2 underwent differentiation and stained strongly with

alizarin red (Fig. 5c) and for alkaline phosphatase (not shown), CD1530-pretreated cells did not (Fig. 5c). As seen in ADTC5 cells (Fig. 4d), CD1530 treatment lowered their steady-state levels of Smad proteins and counteracted their responsiveness to rBMP-2 as indicated by Id1-luc activity (Fig. 5d,e).

To test whether a similar loss of skeletogenic potential was displayed within the *in vivo* environment, the bone marrow-derived MSCs were first grown for 2 to 3 days in monolayer in presence or absence of 100 nM CD1530. The cells were then detached, mixed with Matrigel/rBMP-2 and implanted subcutaneously in nude mice. Because the cells express green fluorescence protein (GFP)<sup>35</sup>, they were readily distinguishable from host cells. Control cells produced conspicuous masses of endochondral bone by 2 weeks that were obvious by  $\mu$ CT and histology and contained numerous GFP- and osteocalcin-positive cells (Fig. 5f, left column). However, the CD1530-pretreated cells largely failed to produce ectopic bone, though they were present in large numbers as revealed by their strong GFP signal (Fig. 5f). Bone volume/total volume quantification showed that the reduction in ectopic bone formation was over 95%.

## DISCUSSION

Here we have shown that RAR $\gamma$  agonists are potent inhibitors of intramuscular and subcutaneous HO and can even mitigate ectopic skeletal tissue formation induced by the constitutively active Q207D<sup>ALK2</sup> mutant. The inhibition of HO appears to be largely irreversible since we observe minimal rebound effects upon stoppage of drug treatment; in addition, the drugs appear to have minimal side effects. Given that chondrogenesis normally requires a drop in retinoid signaling and a concurrent up-regulation of pro-chondrogenic pathways including BMP signaling<sup>15,36</sup>, it is likely that the RAR $\gamma$  agonists elicit their anti-chondrogenic and anti-HO effects by maintaining retinoid signaling active and liganded RAR activity while dampening BMP signaling. Our data indicate also that the latter involves not only an inhibition of Smad phosphorylation, but also a significant proteasome-mediated drop in overall Smad levels and a concurrent reprogramming of the progenitor cells into a non-skeletogenic lineage. Notably, in the recent study using the ALK2<sup>Q207D</sup> transgenic mice, no significant decrease in overall Smad levels was seen following treatment of skeletogenic cells with BMP type I receptor kinase inhibitors<sup>13</sup>, indicating that the RAR $\gamma$  agonists use distinct and more encompassing modes of action and may thus be more potent. Interestingly, liganded RAR $\gamma$  was previously shown to directly interact with Smad proteins and inhibit their function<sup>37</sup>, and we showed previously that liganded RAR $\gamma$  interacts with  $\beta$ -catenin but boosts Wnt/ $\beta$ -catenin signaling<sup>38</sup>. Because Wnt/ $\beta$ -catenin signaling is a potent inhibitor of chondrogenesis<sup>39,40</sup>, it follows that the RAR $\gamma$  agonists probably block chondrogenesis and HO by reciprocally increasing Wnt/ $\beta$ -catenin signaling while decreasing BMP signaling and possibly other pathways<sup>41</sup>. In sum, the RAR $\gamma$  agonists have the biological properties needed to interfere with specific processes and mechanisms needed for HO initiation and progression and may thus represent very effective remedies, likely the most effective reported to date, for this condition and related ectopic ossification conditions<sup>42,43</sup>.



Several notes of caution must be considered before the retinoid agonists can be tested for human therapy. More in depth studies need to be carried out to exclude unwanted side effects. The transient delay in fracture repair seen in RAR $\gamma$  agonist-treated mice could be of concern for patients such as wounded soldiers who may have severe bone fractures. However, these fractures are often subjected to stabilization and traction prior to healing and while inflammation subsides<sup>44</sup>, thus providing a window of opportunity for retinoid treatment and HO prevention. It is to be considered also that the agonists could have negative effects on the growth plate in developing skeletal elements directly or via excess Wnt/ $\beta$ -catenin signaling. If so, this would be a concern for long-term treatment of children with FOP. However, because the RAR $\gamma$  agonists act rapidly and at least in part by diverting the skeletogenic potentials of progenitor cells, it is possible that treatment could be short and/or intermittent and would allow growth plate recovery in between treatment. Lastly, though all the RAR $\gamma$  agonists tested here are very effective, one may be left wondering as to which is the leading candidate towards clinical development. Given its particularly strong activity also seen in our previous study<sup>20</sup>, NRX204647 should be at the top of the list, but this drug has not undergone human testing yet. On the other hand, R667 (also known as Palovarotene) is already in a phase 2 clinical trial for another condition<sup>27</sup> and could thus move toward a clinical trial for HO in an efficient manner.

## METHODS

### *In vitro* chondrogenesis

Limb bud mesenchymal cells isolated from E11.5 wild type, compound RAR $\alpha$ /RAR $\beta$ -deficient or RAR $\gamma$ -null mouse embryos<sup>20</sup> were seeded in high density micromass culture and maintained in DMEM and F12 medium (1:1) containing 3% FBS as described<sup>15</sup>. Cultures were treated with indicated concentrations of all-*trans*-retinoic acid (Sigma) or RAR $\gamma$  agonist NRX 204647 (NuRx Pharmaceuticals); fresh drugs were given with medium change every other day. Parallel control cultures received equal volume of DMSO (vehicle). Cultures were stained with Alcian blue pH1.0 to monitor chondrogenic cell differentiation. Floxed RAR $\alpha$  and RAR $\beta$  mice were mated with Prx1-Cre mice to create the compound RAR $\alpha$ /RAR $\beta$ -deficient limbs. Genotyping procedures and results are shown in Supplementary Fig. 1.

### HO mouse models

Standard muscle trauma-associated HO model was as described<sup>22,45</sup>. Briefly, 3.0 mm x 1.0 mm thick collagen discs were prepared by punched out of collagen sponge sheets (Ultraform<sup>®</sup>, Davol). Five  $\mu$ l aliquots containing 1.0  $\mu$ g of recombinant human BMP-2 (Gene Script Corp.) was adsorbed onto each disc. Longitudinal skin incisions were made on the medial surface of calf muscles in 2 month-old CD-1 female mice. An intramuscular pocket was created microsurgically and one rBMP-2/collagen disc was placed in it; the skin was then closed with 4.0 nylon sutures. The subcutaneous model of HO was created as described<sup>14</sup>. Female mice only were used because they are more easily handled during drug treatment by gavage and can be kept in larger number per cage. For FOP-like HO model, we used the transgenic mice that carry a Cre-inducible constitutively active ALK2<sup>Q207D</sup> mutant and EGFP (CAG-Z-EGFP-caALK2)<sup>13</sup>. To induce HO, 10<sup>8</sup> PFU/10  $\mu$ l of Ad-Cre (Vector

Biolabs) and 0.3  $\mu\text{g}$  per 10  $\mu\text{l}$  cardiotoxin (Sigma) were injected into the left anterior tibial muscles of P7 ALK2<sup>Q207D</sup> mice. To monitor bone formation, 35  $\mu\text{g}$ s per kg body weight Alizarin complexon (Sigma) were injected intra-peritoneally on P29, P31 and P33. GFP and Alizarin signals were captured with a fluorescence stereomicroscope (SZX, Olympus). To test the skeletogenic potentials of RAR $\gamma$  agonist-treated mesenchymal stem cells (MSCs) *in vivo*, we cultured bone marrow-derived GFP-expressing MSCs<sup>35</sup> in monolayer for 2 to 3 days in absence (control) or presence of 100 nM CD1530. Control and CD1530-pretreated GFP-expressing MSCs ( $2.5 \times 10^5$ ) were then mixed with rBMP-2/Matrigel and implanted subcutaneously in host nude mice. All surgical procedures were carried out under anesthesia by inhalation of 1.5% isoflurane in 98.5% oxygen and by following protocols approved by the IACUC.

### Systemic retinoid administration

Stock solutions of retinoids prepared in DMSO were stored at  $-30^\circ\text{C}$  under argon. Just before administration, 30  $\mu\text{l}$  of each stock solution were mixed with 70  $\mu\text{l}$  of corn oil (Sigma) to produce a 100  $\mu\text{l}$  dose/mouse delivered by gavage. Unless otherwise noted, treatment with retinoids started on day 1 from surgery. Companion control mice received vehicle alone (DMSO in corn oil). With regard to the FOP-like transgenic mice, treatment with vehicle or 4 mg per kg body weight per day of CD1530 was started 3 days after Ad-Cre/cardiotoxin injection and continued every other day.

### Soft x-ray and $\mu\text{CT}$ analyses

Tissue samples were fixed in 4% paraformaldehyde at  $4^\circ\text{C}$  and subjected to  $\mu\text{CT}$  analysis using a CT40 scanner (SCANCO) at 55 kV and 70 mA. Data were analyzed at threshold 244 for detection of mineralized component and calculation of bone volume (BV) and then re-analyzed at threshold 110 to measure total sample volume (TV). Normalized bone volume/tissue volume ratios (BV/TV) were calculated by dividing BV with TV and used to calculate differences of experimental versus control values. Soft x-ray images were taken using piXarray100 (Bioptics) in auto-exposure mode.

### Blood tests

Blood samples were collected from heart apex at the moment of sacrifice and stored on ice before centrifugation at  $1000 \times g$  at  $4^\circ\text{C}$  for 10 min to collect serum samples. Samples were then analyzed by VetScan<sup>®</sup> Comprehensive Diagnostic Profile (Abaxis).

### Bone fracture healing

Fibulas were transected with a bone cutter in adult mice under anesthesia and allowed to heal without stabilization. Immediately after surgery and at 2, 4 and 8 weeks after surgery, lateral radiographs of limbs were taken to monitor callus formation and bone healing that were evaluated with a typical fracture healing scoring system: 0, lack of healing; 1, callus formation; 2, onset of bony union; 3, disappearance of fracture line; and 4, complete bony union. Radiographs were scored by two examiners with randomized blinded selection of films.



## Statistical Analysis

Statistical significance of all experiments was determined by one-way factorial ANOVA followed by Bonferroni/Dunn post-hoc multiple comparison tests (Prism 5, GraphPad Software Inc.). *P* values less than 0.01 were considered as statistically significant vs control. All statistical data are presented as means  $\pm$  s.e.m. (*n* = 8).

Other experimental procedures such as histological and immunohistochemical analyses, reporter assay, protein analysis and immunocytochemistry are described in the Supplement.

## Supplementary Material

Refer to Web version on PubMed Central for supplementary material.

## Acknowledgments

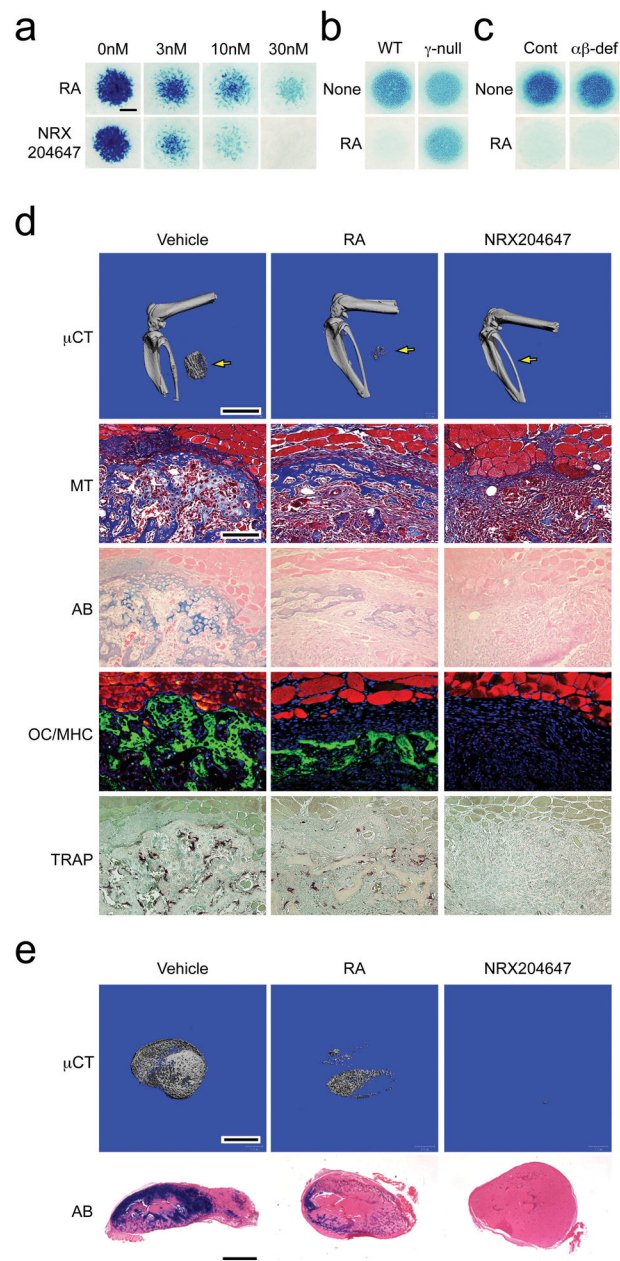
We thank Dr. T. Katagiri (Saitama, Japan) for kindly providing the Id1-luc reporter plasmid, Dr. S. Otsuru and E. Horwitz (Children's Hospital of Philadelphia) for providing the GFP-expressing MSCs and culture methods, and Drs. N. Ghyselinck and P. Chambon (INSERM, Illkirch Cedex, France) for providing the RAR floxed and null mouse lines. This work was supported by contract no. W81XWH-07-1-0212 from the Department of the Army, United States Army Medical Research Acquisition Activity (M.P.) and NIH RO1 grant AR056837 (M.I. and M.P.).

## References

1. Chalmers J, Gray DH, Rush J. Observation on the induction of bone in soft tissues. *J Bone Joint Surg Br.* 1975; 57:36–45. [PubMed: 1090627]
2. Garland DE. A clinical prospective on common forms of acquired heterotopic ossification. *Clin Orthop.* 1991; 263:13–29. [PubMed: 1899635]
3. Nilsson OS, Persson PE. Heterotopic bone formation after joint replacement. *Curr Opin Rheumatol.* 1999; 11:127–131. [PubMed: 10319216]
4. Forsberg JA, et al. Heterotopic ossification in high-energy wartime extremity injuries: prevalence and risk factors. *J Bone Joint Surg.* 2009; 91:1084–1091. [PubMed: 19411456]
5. McCarthy EF, Sundaram M. Heterotopic ossification: a review. *Skeletal Radiol.* 2005; 34:609–619. [PubMed: 16132978]
6. Vanden Booshe L, Vanderstraeten G. Heterotopic ossification: a review. *J Rehabil Med.* 2005; 37:129–136. [PubMed: 16040468]
7. Pignolo RJ, Suda RK, Kaplan FS. The fibrodysplasia ossificans progressiva lesion. *Clin Rev Bone Min Met.* 2005; 5:195–200.
8. Shore E, et al. A recurrent mutation in the BMP type I receptor ACVR1 causes inherited and sporadic fibrodysplasia ossificans progressiva. *Nature Genet.* 2006; 38:525–527. [PubMed: 16642017]
9. Chao ST, Joyce MJ, Suh JH. Treatment of heterotopic ossification. *Orthopedics.* 2007; 30 :457–464. [PubMed: 17598490]
10. Kaplan FS. The medical management of fibrodysplasia ossificans progressiva: current treatment considerations. *Clin Proc Intl Clin Consort FOP.* 2008; 3:1082.
11. Fukuda T, et al. Generation of a mouse with conditionally activated signaling through the BMP receptor, ALK2. *Genesis.* 2006; 44:159–167. [PubMed: 16604518]
12. Zhang D, et al. ALK2 functions as a BMP type I receptor and induces Indian hedgehog in chondrocytes during skeletal development. *J Bone Min Res.* 2003; 18:1593–1604.
13. Yu PB, Deng DY, et al. BMP type I receptor inhibition reduces heterotopic ossification. *Nat Med.* 2008; 14:1363–1369. [PubMed: 19029982]

14. Shimono K, et al. Inhibition of ectopic bone formation by a selective retinoic acid receptor  $\alpha$ -agonist: a new therapy for heterotopic ossification? *J Orthop Res.* 2010; 28:271–277. [PubMed: 19725108]
15. Pacifici M, Cossu G, Molinaro M, Tato' F. Vitamin A inhibits chondrogenesis but not myogenesis. *Exp Cell Res.* 1980; 129:469–474. [PubMed: 7428831]
16. Weston AD, Chandraratna RAS, Torchia J, Underhill TM. Requirement for RAR-mediated gene repression in skeletal progenitor differentiation. *J Cell Biol.* 2002; 158:39–51. [PubMed: 12105181]
17. Weston AD, Hoffman LM, Underhill TM. Revisiting the role of retinoid signaling in skeletal development. *Birth Defects Research Pt C.* 2003; 69:156–173.
18. Rochette-Egly C, Germain P. Dynamic and combinatorial control of gene expression by nuclear retinoic acid receptors (RARs). *Nuclear Rec Signal.* 2009; 7:1–18.
19. Koyama E, et al. Retinoid signaling is required for chondrocyte maturation and endochondral bone formation during limb skeletogenesis. *Dev Biol.* 1999; 208:375–391. [PubMed: 10191052]
20. Williams JA, et al. Retinoic acid receptors are required for skeletal growth, matrix homeostasis and growth plate function in postnatal mouse. *Dev Biol.* 2009; 328:315–327. [PubMed: 19389355]
21. Tacher SM, Vasudevan J, Chandraratna RAS. Therapeutic applications for ligands of retinoic receptors. *Curr Pharmaceut Design.* 2000; 6:25–58.
22. O'Connor JP. Animal models of heterotopic ossification. *Clin Orth Relat Res.* 1998; 346:71–80.
23. Gehin M, et al. Structural basis for engineering of retinoic acid receptor isotype-selective agonists and antagonists. *Chem Biol.* 1999; 6:519–529. [PubMed: 10421757]
24. Keidel S, LeMotte P, Apfel C. Different agonist- and antagonist-induced conformational changes in retinoic acid receptors analyzed by protease mapping. *Mol Biol Cell.* 1994; 14:287–298.
25. Klein ES, et al. Identification and functional separation of retinoic acid receptor neutral antagonists and inverse agonists. *J Biol Chem.* 1996; 271:22692–22696. [PubMed: 8798442]
26. Bernard BA, et al. Identification of synthetic retinoids for selectivity for human nuclear retinoic acid receptor  $\gamma$ . *Biochem Biophys Res Commun.* 1992; 186:977–983. [PubMed: 1323296]
27. Hind M, Stinchcombe S. Palovarotene, a novel retinoic acid receptor gamma agonist for the treatment of emphysema. *Curr Opin Invest Drugs.* 2009; 10:1243–1250.
28. Blaner, WS.; Olson, JA. *The retinoids: Biology, Chemistry, and Medicine.* Sporn, MB.; Roberts, AB.; Goodman, DS., editors. Raven Press; 1994. p. 229-255.
29. Zasloff MA, Rocke DM, Crofford LJ, Hahn GV, Kaplan FS. Treatment of patients who have fibrodysplasia ossificans progressiva with isotretinoin. *Clin Orthop.* 1998; 346:121–129. [PubMed: 9577419]
30. DeSimone DP, Reddi AH. Influence of vitamin A on matrix-induced endochondral bone formation. *Calcif Tissue Int.* 1983; 35:732–739. [PubMed: 6652548]
31. Shen Q, et al. The fibrodysplasia ossificans progressiva R206H ACVRA mutation activates BMP-independent chondrogenesis and zebrafish embryo ventralization. *J Clin Invest.* 2009; 119:3462–3472. [PubMed: 19855136]
32. Korchynskiy O, ten Dijke P. Identification and functional characterization of distinct critically important bone morphogenetic protein-specific response elements in the Id1 promoter. *J Biol Chem.* 2002; 277:4883–4891. [PubMed: 11729207]
33. Massague J. TGF- $\beta$  signal transduction. *Annu Rev Biochem.* 1998; 67:753–791. [PubMed: 9759503]
34. Derynck R, Zhang YE. Smad-dependent and Smad-independent pathways in the TGF- $\beta$  family signaling. *Nature.* 2003; 425:577–584. [PubMed: 14534577]
35. Otsuru S, et al. Osteopoietic engraftment after bone marrow transplantation: effect of inbred strain of mice. *Exp Hematol.* 2010; 38:836–844. [PubMed: 20447443]
36. Hoffman LM, et al. BMP action in skeletogenesis involves attenuation of retinoid signaling. *J Cell Biol.* 2006; 174:101–113. [PubMed: 16818722]
37. Pendaries V, Verrecchia F, Michel S, Mauviel A. Retinoic acid receptors interfere with the TGF- $\beta$ /Smad signaling pathway in a ligand-specific manner. *Oncogene.* 2003; 22:8212–8220. [PubMed: 14603262]

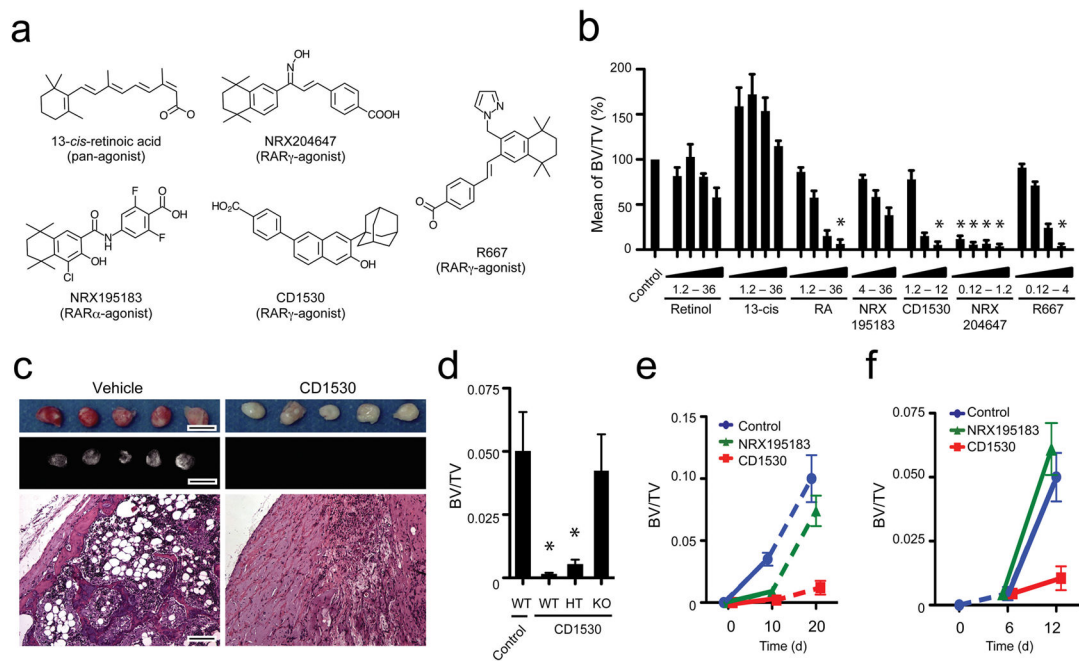
38. Yasuhara R, et al. Wnt/ $\beta$ -catenin and retinoic acid receptor signaling pathways interact to regulate chondrocyte function and matrix turnover. *J Biol Chem.* 2010; 285:317–327. [PubMed: 19858186]
39. Day TF, Guo X, Garrett-Beal L, Yang Y. Wnt/ $\beta$ -catenin signaling in mesenchymal progenitors controls osteoblast and chondrocyte differentiation during vertebrate skeletogenesis. *Dev Cell.* 2005; 8:739–750. [PubMed: 15866164]
40. Tamamura Y, et al. Developmental regulation of Wnt/ $\beta$ -catenin signals is required for growth plate assembly, cartilage integrity, and endochondral ossification. *J Biol Chem.* 2005; 280:19185–19195. [PubMed: 15760903]
41. Nozaki Y, et al. Anti-inflammatory effect of all-trans-retinoic acid in inflammatory arthritis. *Clin Immunol.* 2006; 119:272–279. [PubMed: 16412693]
42. Benglis D, Wang MY, Levi AD. A comprehensive review of the safety profile of bone morphogenetic protein in spine surgery. *Oper Neurosurg.* 2008; 62:423–431.
43. Shao JS, Cai J, Towler DA. Molecular mechanisms of vascular calcification: lessons learned from the aorta. *Arterioscler Thromb Vasc Biol.* 2006; 26:1423–1430. [PubMed: 16601233]
44. Bone LB, Johnson KD, Weigelt J, Scheinberg R. Early versus delayed stabilization of femoral fractures. A prospective randomized study. *J Bone Joint Surg.* 1989; 71 :336–340. [PubMed: 2925704]
45. Kakudo N, Kausumoto K, Wang YB, Iguchi Y, Ogawa Y. Immunolocalization of vascular endothelial growth factor on intramuscular ectopic osteoinduction by bone morphogenetic protein-2. *Life Sci.* 2006; 79:1847–1855. [PubMed: 16857215]



**Figure 1.**

RAR agonists block chondrogenesis and intramuscular rBMP-2-driven HO. **(a)** E11.5 mouse limb mesenchymal cells in micromass cultures were treated with increasing doses of RA or RAR $\gamma$  agonist NRX204647 and were stained with Alcian blue on day 8. **(b)** Similar micromass cultures prepared with E11.5 RAR $\gamma$ -null or wild type (WT) limb mesenchymal cells were treated with RA (100nM) for 8 days. RA inhibited chondrogenesis in WT, but not mutant cultures. **(c)** Micromass cultures prepared with dual RAR $\alpha$ /RAR $\beta$ -deficient or WT limb mesenchymal cells were treated with RA as above. In this case, RA inhibited chondrogenesis in both cultures. **(d)** HO was induced by implantation of rBMP-2-filled collagen sponge into a microsurgically-created pocket inside the calf muscles and the mice

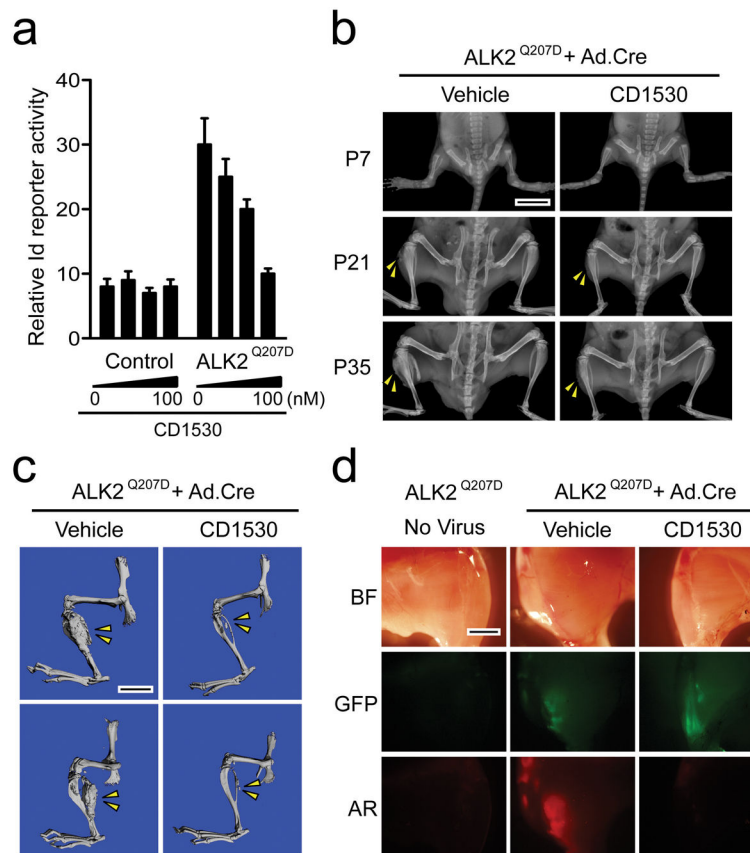
were then treated with vehicle, RA (12 mg per kg body weight per day) or NRX204647 (1.2 mg per kg body weight per day) by gavage. Note the large round mineralized HO masses visible by  $\mu$ CT in vehicle- receiving control mice, their significant decrease in RA-treated mice and their absence in NRX204647-treated mice. Ectopic tissues were sectioned and examined by Masson trichrome (MT) and Alcian blue (AB) staining, immuno-fluorescence detection of myosin heavy chain (MHC: red) and osteocalcin (OC: green), and TRAP staining. Size bar for  $\mu$ CT: 5 mm; and for histology: 200  $\mu$ m. (e) HO was induced by subcutaneous implantation of rBMP-2/Matrigel mixture. Treatment condition and analysis of ectopic tissue were done exactly as above. Bar in  $\mu$ CT panels, 5.0 mm; bar in AB panels, 2.5 mm.



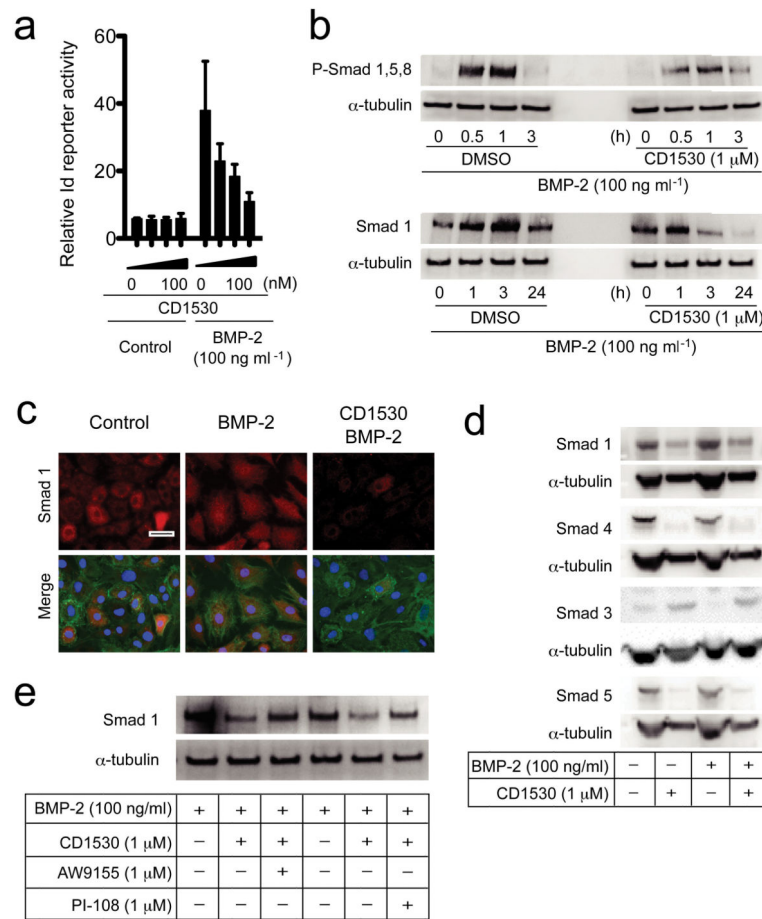
**Figure 2.**

Effectiveness of different retinoids against HO. **(a)** Chemical structures of synthetic RAR $\gamma$  agonists and natural 13-*cis*-RA. **(b)** Suppression of HO by different retinoids was evaluated by measuring bone volume/total volume (BV/TV) in ectopic masses in control versus retinoid-treated mice by  $\mu$ CT on day 12. Values from control groups were set at 100% in each experiment and used to calculate relative values in experimental groups. Each group had a minimum of 8 samples, and data are presented as means average  $\pm$  s.e.m. (\*  $p < 0.01$  vs control). **(c)** Macro views (top), soft x-ray radiograms (middle) and H&E stained histological sections (bottom) of ectopic masses collected from vehicle-treated control and CD1530-treated mice. Bar in top and middle panels, 1.0 cm; and bar in bottom panel, 100  $\mu$ m. **(d)** Selectivity of RAR $\gamma$  agonist action. Subcutaneous HO was triggered in WT, heterozygous RAR $\gamma^{+/-}$  (HT) and RAR $\gamma$ -null (KO) mice, and mice were treated with RAR $\gamma$  agonist CD1530 (4.0 mg per kg body weight per day) or vehicle for 12 days. \*  $p < 0.01$  vs control. **(e)** Evaluation of rebound effects. Mice implanted with rBMP-2/Matrigel mixture subcutaneously were treated with vehicle, CD1530 or RAR $\alpha$  agonist NRX195183 for 10 days. Treatment was stopped, and HO was evaluated by  $\mu$ CT at later time points. **(f)** Window of opportunity tests. Mice implanted as above were left untreated for up to day 6 and were then treated with CD1530 or NRX195183 until day 12.

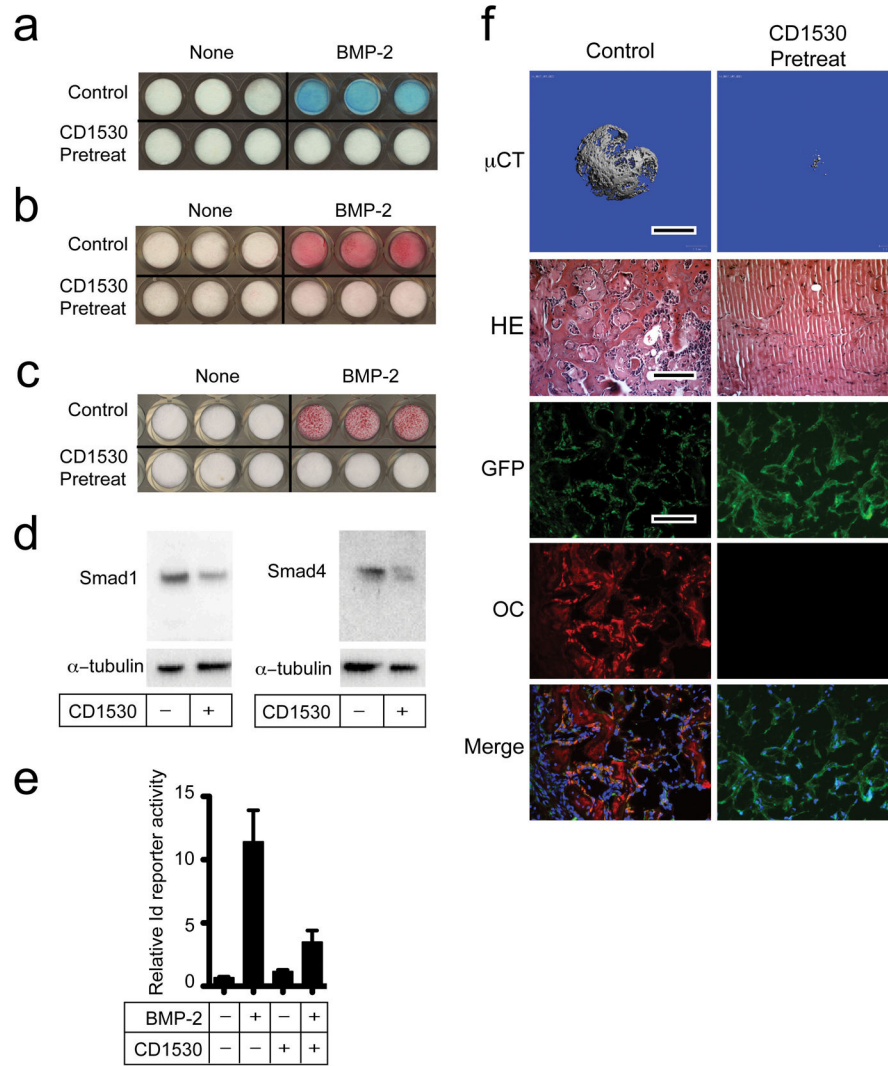


**Figure 3.**

RAR $\gamma$  agonists block FOP-like HO formation. **(a)** ADTC5 cells expressing the strong constitutive-active ALK2<sup>Q207D</sup> or control empty vector were transfected with the BMP signaling reporter Id1-luc and then treated with 0, 10, 30 and 100 nM CD1530. Reporter activity was normalized to pHRG-TK. The strong reporter activity in ALK2<sup>Q207D</sup> expressing cells was counteracted by RAR $\gamma$  agonist treatment. **(b)** ALK2<sup>Q207D</sup> transgenic mouse model of FOP-like HO. Consecutive soft x-ray images of the same Ad-Cre/cardiotoxin-injected mice taken at P7, P21 and P35 showing that massive HO was present in vehicle-treated mice (double arrowheads), but was dramatically reduced in companion CD1530-treated mice (4.0 mg per kg body weight per day). Bar, 1.0 cm. **(c)**  $\mu$ CT images showing that massive HO was present in vehicle-treated Ad-Cre/cardiotoxin-injected ALK2<sup>Q207D</sup> transgenic mice (double arrowheads), but was essentially absent in companion CD1530-treated mice. Bar, 1.0 cm. **(d)** Bright field (BF) and fluorescent images showing that ectopic Alizarin complexon-positive skeletal tissue (AR) had formed in control Ad-Cre/cardiotoxin-injected ALK2<sup>Q207D</sup> transgenic mice receiving vehicle (middle lower panel), but not in those receiving CD1530 (right lower panel). Positive GFP fluorescence verified that Ad-Cre had activated transgene expression in all mice. No GFP and AR fluorescence was seen in mice that had not been injected with Ad-Cre/cardiotoxin (left panels). Bar, 5.0 mm.



**Figure 4.** Mechanisms of RAR $\gamma$  agonist action. **(a)** Id1-luc reporter activity in ATDC5 cells. **(b)** Immunoblots showing that: (i) phosphorylated Smad1/5/8 protein levels were transiently but markedly increased in control (DMSO) ATDC5 cells treated with rBMP-2, but much less in cells treated with CD1530 (top panel); and (ii) overall Smad1 levels did not change in control cells over time, but decreased progressively and markedly in CD1530-treated cells (bottom panel). Membranes were re-blotted with  $\alpha$ -tubulin antibodies for normalization. **(c)** Dual Smad1 and  $\beta$ -actin immunofluorescence staining and nuclear DAPI staining showing that Smad1 was largely cytoplasmic in control cells and relocated to the nucleus during rBMP-2 treatment, but there was minimal detectable Smad1 signal in cells co-treated with CD1530 in either cytoplasm or nucleus. Smad1 is in red,  $\beta$ -actin is in green, and nuclei are in blue. **(d)** Immunoblots similar to those in **(b)** showing that the overall levels of Smad1, Smad4 and Smad5 were all decreased by CD1530 treatment with or without rBMP-2 treatment. **(e)** Immunoblots showing that the decreases in Smad1 levels elicited by CD1530 treatment were significantly counteracted by co-treatment with proteasome inhibitors AW9155 or PI-108.

**Figure 5.**

RAR $\gamma$  agonists reprogram the differentiation potentials of skeletal progenitor cells. **(a-b)** ATDC5 cells were grown in the presence of vehicle (control) or 1  $\mu$ M CD1530 for 2 days, rinsed, re-plated and then grown for an additional 7 days with or without 100 ng ml $^{-1}$  rBMP-2. Note that control cells responded well to rBMP-2 and underwent chondrogenic differentiation revealed by strong Alcian blue **(a)** and alkaline phosphatase **(b)** staining, but the CD1530 pre-treated cells did not and failed to stain. **(c)** Similar experiments with GFP-expressing mouse bone marrow-derived MSCs show that the cells underwent differentiation upon rBMP-2 treatment (top row), but CD1530 pre-treated MSCs did not and failed to stain with alizarin red (bottom row). **(d)** Immunoblots showing the steady state levels of Smad1 and Smad4 in MSCs treated without (-) or with (+) 1  $\mu$ M CD1530 for 12 hr. **(e)** Id1-luc reporter activity in control MSCs treated with or without rBMP-2 in the presence or absence of CD1530. **(f)** Control and CD1530-pretreated GFP-expressing MSCs were mixed with rBMP-2/Matrigel and implanted in nude mice subcutaneously, and ectopic tissue masses were analyzed by  $\mu$ CT, H&E staining, osteocalcin (OC) immunostaining and GFP

fluorescence signal. Merged images of GFP and OC images are shown at the bottom. Bar in top panel, 5.0 mm; bar in second panel, 250  $\mu\text{m}$ ; and bar in third panel, 150  $\mu\text{m}$ .

Author Manuscript

Author Manuscript

Author Manuscript

Author Manuscript